Spherical Nanoporous Assemblies of Iso-Oriented Cobalt Ferrite Nanoparticles: Synthesis, Microstructure, and Magnetic Properties

C. Cannas,* A. Ardu, A. Musinu, D. Peddis, and G. Piccaluga

Dipartimento di Scienze Chimiche, Università di Cagliari, Cittadella Universitaria di Monserrato, Cagliari, 09042

Received April 16, 2008

Nanoporous spherical assemblies of iso-oriented cobalt ferrite nanoparticles with a high surface area were prepared via a normal micelles process. The spherical magnetic assemblies were coated with a silica layer through an inverse micelles route. The microstructure and morphology were studied by X-ray diffraction, transmission electron microscopy and N_2-physisorption techniques. The primary $CoFe_2O_4$ nanocrystalline particles (~7 nm) assemble into spherical nanoporous aggregates with an average size of about 50−60 nm and the coating process leads to core−shell nanostructures with an amorphous 7−8 nm thick silica shell that covers the spherical assemblies homogeneously. The magnetic properties of both uncoated and silica-coated nanostructures were also investigated.

Introduction

Magnetic nanoparticles (MNp) with high magnetization values have found a wide range of biomedical applications, both in vivo and in vitro, (e.g., drug targeting, hyperthermia, and magnetic separation) and are also used for diagnostic purposes, e.g., enhancing the contrast of magnet resonance image (MRI).[1−3] Although magnetic particles with a narrow size distribution have been synthesized through various methods,[4−10] the products are overwhelmingly dominated by particles smaller than 30 nm. However, for many purposes, it is preferable to fabricate nanoparticle assemblies of about 100 nm, rather than small nanoparticles, because they can be easily moved by an ordinary external magnetic device.[11] It is therefore an interesting challenge to develop approaches to assembling magnetic nanoparticles with suitable sizes (from 30 to 100 nm) and morphology without compromising the surface area, in order to meet the special need of biomedical fields.

Assembling nanoparticles into highly ordered materials is a potential bottom-up approach to creating advanced artificial materials with distinct micro and nanostructures (electronic, optical, or magnetic nanodevices with high performances) and is a clue toward the understanding of the growth mechanism of crystals. Therefore, the knowledge of the factors that govern the creation of the assembly of nanoparticles is essential to optimize the functional properties of the nanostructures in a precise manner.

The realization of assemblies of nanoparticles with advanced functions requires the development of new and efficient approaches toward combining the very small building blocks into desired structures. Up to now, several methods have been developed to fabricate various superstructures from primary nanoparticles,[12−19] among which, in particular, a number of methods based on surfactant-assisted strategy. In some cases, however, for many purposes, the preparation and removal of the surfactant are difficult tasks. In these methodologies, primary nanoparticles self-assemble through noncovalent interactions, creating a secondary architecture whose properties greatly depend on their building blocks. The control of the morphology and the properties of nanocrystals is expected to influence those of their own assemblies, that in turn can, in principle, be tuned to meet specific needs.

Co_3O_4 spheres with oriented assembly of nanoparticles have been obtained by He at. al[13] through a surfactant-assisted solvothermal synthesis. Sodium dodecylbenzenesulfonate added to a suspension containing $Co(NO_3)_2$ and water in absolute methanol led to the aggregation of the primary nanoparticles into iso-oriented spherical assemblies with open nanopores. The solvent and the water content have

* Corresponding author. E-mail: ccannas@unica.it.

(1) Pankhurst, Q. A.; Connolly, J.; Jones, S. K.; Dobson, J. *J. Phys. D: Appl. Phys.* **2003**, *36*, R167.
(2) Tartaj, T.; Puerto Morales, M.; Veintemillas-Verdaguer, S.; Gonzàlez-Carreño, T.; Serna, C. J. *J. Phys. D: Appl. Phys.* **2003**, *36*, R182.
(3) Gupta, A. K.; Gupta, M. *Biomaterials* **2005**, *26*, 3995.
(4) Feltin, N.; Pileni, M. P. *Langmuir* **1997**, *13*, 3927.
(5) Vestal, C. R.; Zhang, Z. J. *Int. J. Nanotechnol.* **2004**, *1*, 240.
(6) Vargas, J. M.; Zysler, R. D. *Nanotechnology* **2005**, *16*, 1474.
(7) Machala, L.; Zboril, R.; Gedanken, A. *J. Phys. Chem. B* **2007**, *111*, 4003.
(8) Matijevic, E. *Chem. Mater.* **1993**, *5* (4), 412.
(9) Hyeon, T.; Lee, S. S.; Park, J.; Chung, Y.; Na, H. B. *J. Am. Chem. Soc.* **2001**, *123*, 12798.
(10) Mathew, D. S; Juang, R. S. *Chem. Eng. J* **2007**, *129*, 51.
(11) Xia, H. B.; Yi, J.; Foo, P. S.; Liu, B. *Chem. Mater.* **2007**, *19*, 4087.
(12) He, T.; Chen, D.; Jiao, X. *Chem. Mater.* **2004**, *16*, 737.
(13) He, T.; Chen, D.; Jiao, X.; Xu, Y.; Gu, Y. *Langmuir* **2004**, *20*, 8404.
(14) Wang, H.; Miao, J. J.; Zhu, J. M.; Ma, H. M.; Zhu, J. J.; Chen, H. Y. *Langmuir* **2004**, *20*, 11738.
(15) Ewers, T. D.; Sra, A. K.; Norris, B. C.; Cable, R. E.; Cheng, C. H.; Shantz, D. F.; Schaak, R. E. *Chem. Mater.* **2005**, *17*, 514.
(16) Hussain, I.; Wang, Z.; Cooper, A. I.; Brust, M. *Langmuir* **2006**, *22*, 2938.
(17) Jia, B.; Gao, L. *J. Phys. Chem. C* **2008**, *112*, 666.
(18) Yu, D.; Sun, X.; Zou, J.; Wang, Z; Wang, F.; Tang, K. *J. Phys. Chem. B.* **2006**, *110*, 21667.
(19) Euliss, L. E.; Grancharov, S. G.; O'Brien, S.; Deming, T. J.; Stucky, G. D.; Murray, C. B.; Held, G. A. *Nano Lett.* **2003**, *3* (11), 1489.

10.1021/cm801839s CCC: $40.75
Published on Web 09/24/2008

an important role on the phases and morphology of the products. An efficient approach toward the fabrication of spherical aggregates of anatase nanocrystals has been reported by Wang et al.[14] The synthesis is based on the controlled hydrolysis of titanium (IV) sulfate in acidic media in the presence of a cationic surfactant, cetyltrimethylammonium bromide (CTAB) in cyclohexane. The interaction between cyclohexane microdroplets and the CTAB self-assemblies led to the assembly of 4−5 nm sized anatase nanocrystals into spherical aggregates with wormhole-like mesoporous structure. Assemblies of 1−3 nm sized rhodium nanoparticles into spherical aggregates have also been prepared by Ewers et al.[15] through the reduction of $RhCl_3$ with $NaBH_4$ in presence of poly(vinyl pyrrolidone) PVP. The interaction between PVP and sodium dodecylsulfate was exploited in order to modulate the spherical aggregate size. The cooperative assembly of maghemite nanoparticles into spherical assemblies in the presence of amino-acid-based polymers has been studied by Euliss et al.[19] They demonstrated that electrostatic interactions between block copolypeptides and nanoparticles can control the organization of these components and declared that by altering the composition of the block copolypeptide, it should be possible to control both the size and the stability of the resulting dispersed nanoparticle spherical clusters.

Oxide-based spinel ferrites, in particular iron oxides like maghemite and magnetite, have been widely used in biomedicine and are very promising because of their well-known biocompatibility.[1−3] However, the use of different materials with larger magnetic anisotropy and larger magnetic moments is envisioned. This would allow a significant improvement on material efficiency, in particular for magnetic fluid hyperthermia.

Recently, some works have been published on self-assembling methods for the preparation of magnetic metal oxide nanoparticles;[11,17−19] but, to the best of our knowledge, none of them has been devoted to cobalt ferrite spherical assemblies.

Spinel cobalt ferrite nanoparticles have been extensively studied because they form a magnetic system which is an ideal candidate toward understanding and controlling magnetic properties at the atomic level through chemical manipulation.[20−25] $CoFe_2O_4$ has also been proposed for biomedical applications[26,27] because of its known large anisotropy compared to other oxide ferrites.[28−30] However, its use in medicine is restricted because of numerous problems such as toxicity due to the remarkable amount of cobalt release in aqueous solutions, aggregation in solution, and poor accessibility of the surface when surfactants are used.[30] Therefore, the magnetic nanoparticles need to be coated with a compatible, nontoxic, and water-stable dispersing material. From this point of view, encapsulating magnetic nanoparticles in silica is a promising and important approach in the development of magnetic nanoparticles for technological and biomedical applications and has been widely used to coat single or multiple (2−3 units) core nanoparticles.[31−41] The rich and well-documented chemistry of biocompatible silica colloids may allow a practical implementation of magnetic nanoparticles in magnetically guided drug delivery, tumor targeting, and magnetically assisted chemical separation of cell and/or proteins. The silica shell certainly provides a chemically inert surface for the nanoparticulate system in biological media. Moreover, it greatly improves the wettability and can easily be surface-modified to link molecules with interesting biofunctionalities.

In this work, we present the achievement of highly porous and monodispersed $CoFe_2O_4$ spherical assemblies of about 50−60 nm made up of small primary nanoparticles. The spherical assemblies have been coated with silica. Normal micelles have been used to prepare the cobalt ferrite nanoparticles, and an inverse (w/o) micelles route has been used for the coating process with silica. The interactions among magnetic nanoparticles are a decisive factor for their application in medicine and biotechnology; for this reason magnetic characterization has been performed both on the uncoated and coated samples.

Experimental Section

Synthesis. *$CoFe_2O_4$ Nanoparticles.* $CoFe_2O_4$ nanoparticles were synthesized through the formation of normal micelles using sodium dodecyl sulfate (SDS) as surfactant,[4,5,10] following a procedure similar to that proposed by Pileni et al.[4] and Zhang et al.[5]

(20) Hutlova, A.; Niznansky, D.; Rehspringer, J. L.; Estournès, C.; Kurmoo, M. *Adv. Mater.* **2003**, *15* (19), 1622.
(21) Shafi, K. V. P. M.; Gedanken, A.; Prozorov, R.; Balogh, J. *Chem. Mater.* **1998**, *10*, 3445.
(22) Rondinone, A. J.; Samia, A. C. S.; Zhang, Z. J. *J. Phys. Chem. B* **1999**, *103*, 6876.
(23) Cannas, C.; Musinu, A.; Piccaluga, G.; Fiorani, D.; Peddis, D. *Chem. Mater.* **2006**, *18* (16), 3835.
(24) Cannas, C.; Musinu, A.; Piccaluga, G.; Fiorani, D.; Peddis, D.; Rasmussen, H. K.; Morup, S. *J. Chem. Phys.* **2006**, *125*, 164714.
(25) Peddis, D.; Cannas, C.; Musinu, A.; Piccaluga, G. *J. Phys. Chem. C* **2008**, *112* (13), 5141.
(26) Kückelhaus, S.; Reis, S. C.; Carneiro, M. F.; Tedesco, A. C.; Oliveira, D. M.; Lima, E. C. D.; Morais, P. C.; Azevedo, R. B.; Lacava, Z. G. M. *J. Magn. Magn. Mater.* **2004**, *272*, 2402.
(27) Baldi, G.; Bonacchi, D.; Innocenti, C.; Lorenzi, G.; Sangregorio, C. *J. Magn. Magn. Mater.* **2007**, *311*, 10.
(28) Tung, L. D.; Kolesnichenko, V.; Caruntu, D.; Chou, N. H.; O'Connor, C. J.; Spinu, L. *J. Appl. Phys.* **2003**, *93*, 7486.
(29) Hanh, N.; Quy, O. K.; Thuy, N. P.; Tung, L. D.; Spinu, L. *Physica B* **2003**, *327*, 382.
(30) Pillai, V.; Shah, D. O. *J. Magn. Magn. Mater.* **1996**, *163*, 243.
(31) Mornet, S.; Grasset, F.; Portier, J.; Duguet, E. *Eur. Cells Mater.* **2002**, *3*, 110.
(32) Yi, D. K.; Selvan, S. T.; Lee, S. S.; Papaefthymiou, G. C.; Kundaliya, D.; Ying, J. Y. *J. Am. Chem. Soc.* **2005**, *127*, 4990.
(33) Yi, D. K.; Lee, S. S.; Papaefthymiou, G. C.; Ying, J. Y. *Chem. Mater.* **2006**, *18*, 614.
(34) Deng, Y. H.; Wang, C. C.; Hu, J. H.; Yang, W. L.; Fu, S. K. *Colloids Surf., A* **2005**, *262*, 87.
(35) Tada, D. B.; Vono, L. L. R.; Duarte, E. L.; Itri, R.; Kiyohara, P. K.; Baptista, M. S.; Rossi, L. M. *Langmuir* **2007**, *23*, 8194.
(36) Caruso, F.; Spasova, M.; Susha, A. M.; Giersig; Caruso, R. A. *Chem. Mater.* **2001**, *13*, 109.
(37) Grasset, F.; Labhsetwar, N.; Li, D.; Park, D. C.; Saito, N.; Haneda, H.; Cador, O.; Roisnel, T.; Mornet, S.; Duguet, E.; Portier, J.; Etourneau, J. *Langmuir* **2002**, *18*, 8209.
(38) Lu, C. W.; Hung, Y.; Hsiao, J. K.; Yao, M.; Chung, T. H.; Lin, Y. S.; Wu, S. H.; Hsu, S. C.; Liu, H. M.; Mou, C. Y.; Yang, C. S; Huang, D. M; Chen, Y. C. *Nano Lett.* **2007**, *7, 1*, 149.
(39) Shukoor, M. I.; Natalio, F.; Therese, H. A.; Tahir, M. N.; Ksenofontov, V.; Panthöfer, M.; Eberhardt, M.; Theato, P.; Schröder, H. C.; Müller, W. E. G.; Tremel, W. *Chem. Mater.* **2008**, *20*, 3567.
(40) Philipse, A. P.; van Bruggen, M. P. B.; Pathmamanoharan, C. *Langmuir* **1994**, *10*, 92.
(41) Salgueiriño-Maceira, V.; Spasova, M.; Farle, M. *Adv. Funct. Mater.* **2005**, *15*, 1036.

Aqueous solutions containing $CoCl_2$ $6H_2O$ (Aldrich, 98%) and $FeCl_2$ $4H_2O$ (Aldrich, 98%) in a 1:2 molar ratio were added to an aqueous solution of SDS (Aldrich, 98%) and stirred constantly, at room temperature, for 30 min to form probably hydrated $Co_xFe_{1-x}(DS)_2$ mixed micelles. To avoid the possible precipitation of iron hydroxides, an amount of SDS greater than the stoichiometric one was used. This micellar solution was kept in a bath, at 80 °C, in constant mechanical stirring; methylamine solution, heated at the same temperature, was added. The solution became green, and after a few minutes, the color changed to dark brown. The dark slurry was stirred for 3 h and then cooled to room temperature. The precipitate was isolated by decantation and centrifugation. The nanoparticles were washed with diluted ammonia to remove the surfactant excess. To take the surfactant completely away, the powder was submitted to several cycles of washing and centrifugation. Finally the $CoFe_2O_4$ powder was dried overnight in an oven at 70−80 °C.

Silica-Coated $CoFe_2O_4$ Spheres. Nanoparticles silica coating was performed through the formation of water in cyclohexane reverse microemulsion.[33,42] In a typical synthesis, polyoxyethylene(5)-nonylphenyl ether (IGEPAL CO-520, 0.025 mol) was dispersed in 500 mL of cyclohexane and added to a concentrated ammonia dispersion of $CoFe_2O_4$ nanoparticles (28,6 mg/mL)) previously sonicated for 15 min. The resulting mixture was at first submitted to 30 min of sonication and then to a vigorous stirring. Tetraethylorthosilicate (TEOS, Aldrich 98%, 3 mL) was added, and the reaction was allowed to proceed at room temperature for five days, under continuous stirring, in order to favor the exchange of the surfactant with TEOS and the subsequent transfer to the hydrophilic phase. The particles were collected by a magnet, and the cyclohexane supernatant was decanted. The powder was washed with methanol and water several times to obtain the final silica-coated $CoFe_2O_4$ sample. Because of the presence of negative charges on the surface of the silica shell, these magnetic nanoparticles, having a core−shell structure, form a stable dispersion in water without using other surfactants. The ratio between the concentration of cobalt ferrite nanoparticles and TEOS has to be optimized in order to avoid the homogeneous nucleation of silica, and thus the formation of core-free silica spheres. Although several parameters (such as growth time and the concentration of ammonia catalyst or water) could be employed to control the thickness of the silica shell, we found it most convenient and reproducible to adjust the shell thickness by changing the concentration of the TEOS precursor.

Characterization Techniques. The samples were characterized by XRD, using a Seifert diffractometer with a $\theta-\theta$ Bragg−Brentano geometry with Cu Kα wavelength.

The mean dimension, D, of crystallites was obtained by Scherrer's equation

$$\langle D \rangle = K\lambda/\beta\cos\theta \qquad (1)$$

by elaborating the most intense X-ray peaks through Origin Software using the PseudoVoigt function to fit the peaks and to extrapolate β and Θ. In eq 1, K is a constant related to the crystallite shape (0.9), β is the pure breath of the powder reflection free of the broadening due to instrumental contributions. This calibration was performed by means of the spectrum of a standard Si sample and using the Warren correction $\beta_{sample} = (\beta_{exp}^2 - \beta_{std}^2)^{1/2}$.

Finely ground samples were dispersed in octane and submitted to an ultrasonic bath. The suspensions were then dropped on carbon-coated copper grids for the TEM observations. Cobalt-ferrite nanoparticles were observed in electron micrographs obtained with a TEM (JEOL 200CX), operating at 200 kV. High-resolution TEM images were obtained with a JEM 2010 UHR equipped with a Gatan Imaging Filter (GIF) with a 15 eV window and a 794 slow scan CCD camera. Average particle size was obtained by measuring the average diameter of a number of particles close to 100 in different parts of the grid.

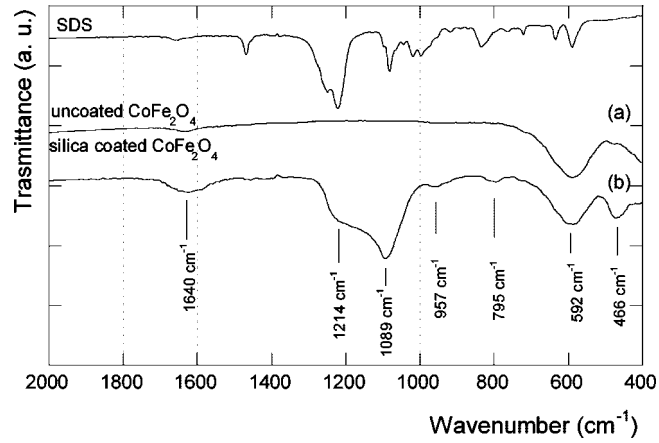

Figure 1. FTIR spectra of the (a) uncoated and (b) silica-coated $CoFe_2O_4$ sample and SDS as a reference.

IR spectra were collected in the Mid region from 400 to 2000 cm^{-1}, using a Bruker Equinox 55 spectrophotomer on KBr pellets.

Textural analysis was carried out on a Sorptomatic 1990 System (Fisons Instruments, Rodano (Mi), Italy) by determining the nitrogen adsorption/desorption isotherms at 77 K. Before analysis, the samples were heated under a vacuum at 50 °C overnight. In the case of mesoporous samples, the specific surface was assessed by the Brauner Emmett Teller (BET) method.

DC measurements of magnetic moment were performed by a Quantum Design SQUID magnetometer, equipped with a superconducting magnet able to produce fields up to 5 T. The samples in the form of powder were immobilized in epoxy resin to prevent any movement of nanoparticles. Thermal dependence of magnetization was studied according to zero-field-cooled (ZFC) and field-cooled protocols (FC). ZFC magnetization (M_{ZFC}) was measured by cooling samples in a zero magnetic field and then by increasing the temperature in an applied field of 5 mT, whereas FC magnetization (M_{FC}) was recorded by cooling the samples in the same field of 5 mT.

Results

Uncoated $CoFe_2O_4$ Particles. FT-IR analysis (Figure 1) was performed to study the efficiency of washing procedures in removing the SDS surfactant. Toward this end, the IR spectrum of the uncoated $CoFe_2O_4$ sample (Figure 1a) is compared with the spectrum of SDS. Two large bands are present at about 1640 and 590 cm^{-1} respectively, because of the bending of the adsorbed water molecules and to the stretching of Me−O in tetrahedral sites, typical of the cobalt ferrite phase.[43] The typical stretching and bending adsorptions of the OSO_3^- group of the SDS surfactant [44,45] are not present, indicating that the washing procedure is efficient.

The X-ray diffraction pattern of the synthesized powder is represented in Figure 2a; Bragg reflections in the 2θ range of 10−70° can be indexed to be a single $CoFe_2O_4$ phase

(42) Vestal, C. R.; Zhang, Z. J. *Nano Lett.* **2003**, *3* (12), 1739.
(43) Gillot, B.; Jemmali, F.; Rousset, A. *J. Solid State Chem.* **1983**, *50*, 138.
(44) Sperline, R. P. *Langmuir* **1997**, *13*, 3715.
(45) Valentim, I. B.; Joekes, I. *Colloids Surf., A* **2006**, *290*, 106.

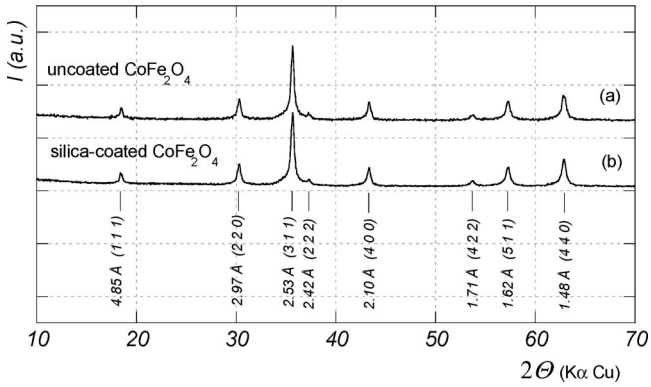

Figure 2. XRD patterns of the (a) uncoated and (b) silica-coated $CoFe_2O_4$ sample.

with a cubic spinel structure (PDF Card 22−1086). No peaks of any other phase are detected. According to the Debye−Scherrer formula, an average crystallite size of about 21 ± 1 nm is derived from the half-height breadth of the most intense peaks.

Figure 3a shows representative TEM micrographs of the $CoFe_2O_4$ powder. It can be clearly seen that spherical particles of about 50−60 nm in size were fabricated. These spherical aggregates are present and stably keep their shape and size unchanged also after the washing procedures, the complete elimination of surfactant, the dispersion in water, in concentrated ammonia or after the treatment with some acids.

The images at higher-magnification (images b and c in Figure 3) and in high-resolution mode (images d and f) show that the spherical particles are made of about 7 nm primary nanocrystals and a wormlike nanopore structure with pore size of about 2−3 nm. The high-resolution energy-filtered TEM (EFTEM) image (Figure 3d) shows a single aggregate, where the parallel lattice fringes are uniformly extended over the primary building blocks, the grain boundaries, and the nanopores. It can be clearly seen that the nanoparticles are organized into an iso-oriented attachment structure through sharing identical lattice planes. The lattice plane distance of 4.8 Å was calculated from the image (Figure 3d), which corresponds to the (111) reflex of the cubic $CoFe_2O_4$ phase. The iso-oriented structure is further confirmed by the FFT image (Figure 3e) that shows symmetrically aligned spots like satellite reflections caused by double diffraction.

The image at a higher magnification (Figure 3f) reveals that the primary particles have a cubic shape, and a more careful observation shows that two or three particles share corners, edge, or faces to form twin crystals, which is consistent with the symmetrical double spots present in the FFT (Figure 3e).

Figure 4 shows N_2 adsorption−desorption isotherms of the $CoFe_2O_4$ powder. One can observe that, besides the mesopores produced by interaggregated spherical particles (at $0.8 < P/P_0 < 1.0$), the BJH pore size distribution indicates mesopores formed among the primary nanoparticles within the aggregates with sizes centered at about 2−3 nm (Figure 4 inset), consistent with TEM results. The surface area of the $CoFe_2O_4$ aggregates is 160 m^2/g, as calculated by the linear part of the BET plot, and the total pore volume at $P/P_0 = 0.98$ is 0.40 cm^3/g. The surface area (among the highest reported in literature for $CoFe_2O_4$ powders) and the large volume support the fact that the $CoFe_2O_4$ aggregated particles have a nanoporous structure.

The high BET specific surface area, calculated according to the equation

$$d_{BET} = \frac{6}{\rho(SSA)}$$

(where d_{BET} is the BET particle size, ρ is the theoretical density of the material, and SSA is the specific surface area) is in good agreement with the theoretical value calculated by assuming dense and regular $CoFe_2O_4$ cubes with edge of 7 nm (ρ = bulk material theoretical density = 5.20 g/cm^3). This is an important indication of the absence of intraparticle porosity and also that crystal twinning takes place through the sharing of edges instead of faces.

ZFC-FC curves of the spherical aggregates, reported in figure 5a, show a magnetic behavior which can be interpreted according to TEM observations. The curves are not yet superposing at T = 325K, indicating the presence of nanoparticles still in a ferrimagnetic state at room temperature.[46] Between 240 and 100 K, the FC magnetization decreases with the lowering of temperature, and a constant trend is observed below 100 K. This behavior can be ascribed to strong nanoparticles interactions that lead to a collective magnetic order state with high anisotropy,[47,48] as expected for iso-oriented magnetic oxide nanoparticles.

Figure 6 (left side) shows the hysteresis loop recorded at 5K. In table 1 saturation magnetization (M_s), coercive field (H_c) and reduced remanent magnetization (M_r/M_s) are reported. The H_c value is higher than in bulk ferrite, but lower than those reported in the literature for cobalt ferrite nanoparticles.[49,24] Once more, this can be ascribed to the presence of strong magnetic interaction among nanoparticles which is consistent with Néel[50] and Wohlfarth[51] theories. The M_s value is close to that ascribed to cobalt ferrite nanoparticles[49,52] and lower than those reported for the corresponding bulk material (85−93 A m^2 Kg^{-1}).[24] The saturated character observed in hysteresis curves suggests that spin canting effects do not have an important role in the lowering of M_s, which could then be ascribed to a variation of inversion degree.[52]

The reduced remanence magnetization shows a higher value than that expected for random assemblies of monodomain nanoparticles with uniaxial anisotropy (0.5).[53] This can be due to different effects, such as cubic anisotropy,[53] or iso-oriented aggregation of nanoparticles, as evidenced by HRTEM. Interacting $CoFe_2O_4$ nanoparticles prepared with

(46) Morrish, A. H., *The Physical Principles of Magnetism*; John Wiley & Sons: New York, 1965; p 394.
(47) Zysler, R. D.; Fiorani, D.; Testa, A. M. *J. Magn. Magn. Mater.* **2001**, *224*, 5.
(48) Hanson, M.; Johanson, C.; Pedersen, M. S.; Morup, S. *J. Phys.: Condens. Matter* **1995**, *7*, 9269.
(49) Grigorova, M.; Blythe, H. J.; Blaskov, V.; Rusanov, V.; Pektov, V.; Mesheva, V.; Nihtianova, D.; Martinez, Ll. M.; Muñoz, J. S.; Mikhov, M. *J. Magn. Magn. Mater.,* **1998**, *183*, 163.
(50) Nèel, L. C. R. *Acad. Sci. Paris* **1947**, *224*, 1550.
(51) Wohlfart, E. P. *Proc. R. Soc. London, Ser. A* **1955**, *232*, 208.
(52) Cannas, C.; Falqui, A.; Musinu, A.; Peddis, D.; Piccaluga, G. *J. Nanopart. Res.* **2006**, *8*, 255.
(53) Moumen, N.; Bonville, P.; Pileni, M. P. *J. Phys. Chem. B* **1996**, *100*, 14410.

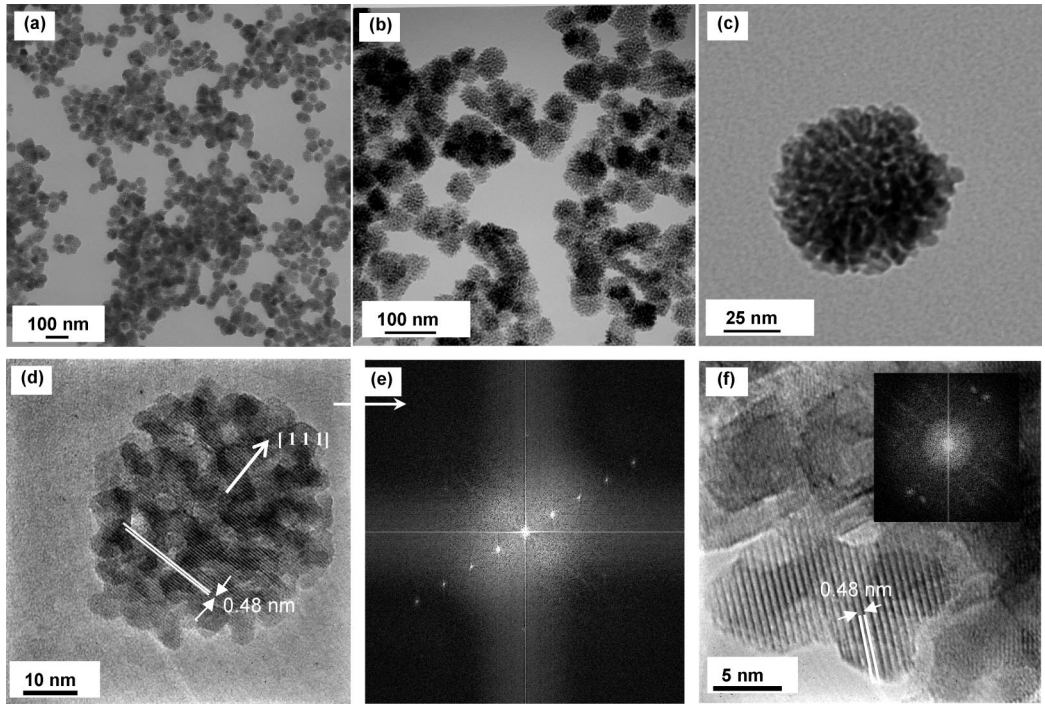

Figure 3. (a−c) TEM images, (d, f) EFTEM images, and (e, and inset) corresponding FFT of the uncoated $CoFe_2O_4$ sample.

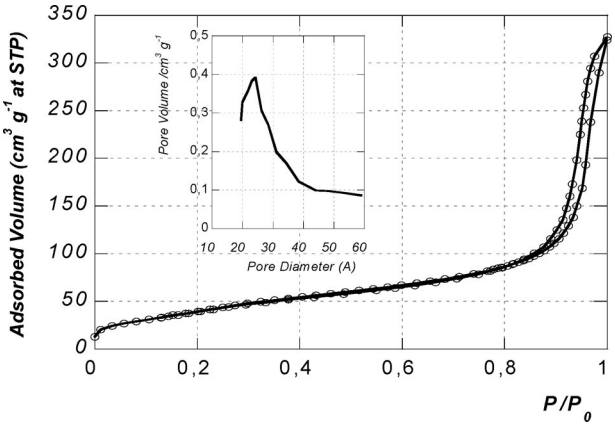

Figure 4. Nitrogen physisorption isotherms and pore size distribution (inset) of the uncoated $CoFe_2O_4$ sample.

a similar method, but not organized in spherical iso-oriented aggregates, show similar magnetic properties but a lower M_r/M_s value ($M_r/M_s = 0.67$).[42] This seems to suggest that the assembly in iso-oriented clusters can give an important contribution in the increasing of M_r/M_s values in our samples.

Silica-Coated Particles. Besides the absorption peaks of the uncoated samples, the FTIR spectrum (Figure 1b) of the silica-coated sample reveals the bands at 1214, 1084, 957, and 795 cm^{-1}, which is typical of the well-formed amorphous sol−gel silica.[54,55] The bands associated with cobalt ferrite fall at the same value as that found for the uncoated sample; this indicates that the coating process does not have any evident effect on the structure and on the surface of the nanoparticles, which in turn suggests the absence of strong interactions of the magnetic core with the silica shell. X-ray diffraction pattern for the cobalt ferrite particles after silica coating is represented in Figure 2b and compared with the uncoated sample. Bragg reflections remain identical before and after silica coating, indicating that the silica shell is amorphous and the crystallinity of the magnetic nanoparticulate core is retained after the coating procedure. Debye−Scherrer calculations predict a value of 21 ± 1 nm for the average crystallite size, equal within the experimental error to that of the uncoated sample. The size and shape of cobalt ferrite spherical assemblies are retained during the silica coating, as shown in a typical TEM image (Figure 7a). The spherical assemblies are homogeneously covered by a 7−8 nm thick silica shell (Figure 7b). The coating process does not even affect the peculiar properties of the aggregate, which, in fact, presents iso-oriented planes as shown in Figure 7c and in its FFT (Figure 7d), even after the coating.

ZFC-FC curves of the coated sample are shown in figure 5b. The similar trend of the curves of the uncoated and silica-coated samples indicates that strong magnetic interactions among particles exist even when they are protected by silica. Considering the efficient coating procedure, this result suggests that the interaggregates interactions are very low, whereas the intra-aggregate interactions play a major role in the physics of these systems.

Figure 6 (right side) shows a hysteresis loop recorded at 5K. In table 1 saturation magnetization (M_s), coercive field (H_c) and reduced remanent magnetization are reported. Taking into account the error associated with the H_c values, the results are quite similar for both samples. The saturation magnetization and the remanent magnetization decrease after silica coating, and this is mainly because of the lower amount of magnetic material per mass. In fact, because IR measurements show that there are no strong interactions between the silica shell and the magnetic core as a consequence of

(54) Bruni, S; Cariati, F.; Casu, M.; Lai, A.; Musinu, A.; Piccaluga, G.; Solinas, S. *Nanostruct. Mater.* **1999**, *11* (5), 573.
(55) Casu, M.; Lai, A.; Musinu, A.; Piccaluga, G.; Solinas, S. *J. Mater. Sci.* **2001**, *36*, 3731.

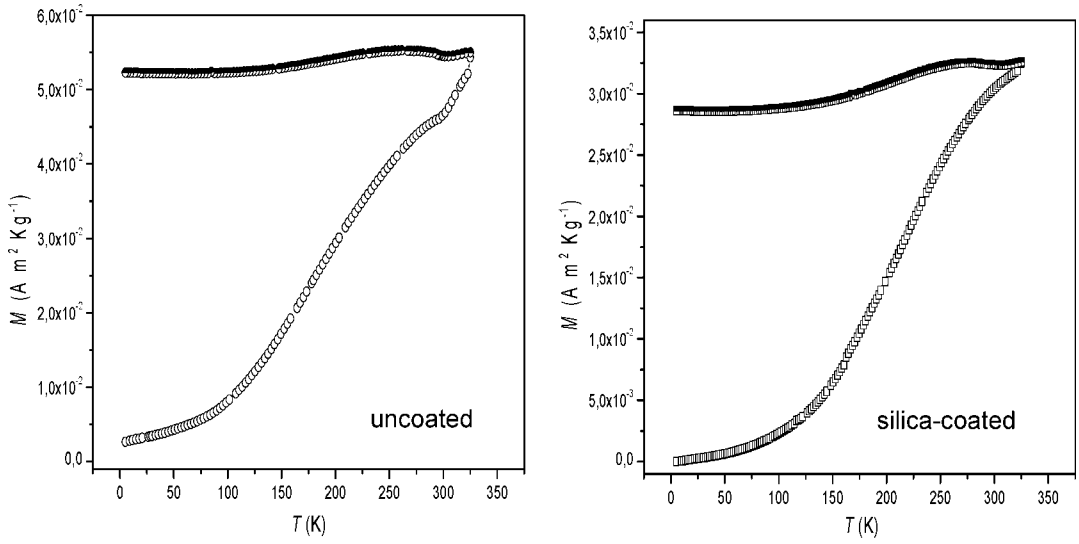

Figure 5. ZFC and FC curves of the uncoated (left side) and coated (right side) $CoFe_2O_4$ sample. For each pair of curves, the upper one is the FC and the lower the ZFC.

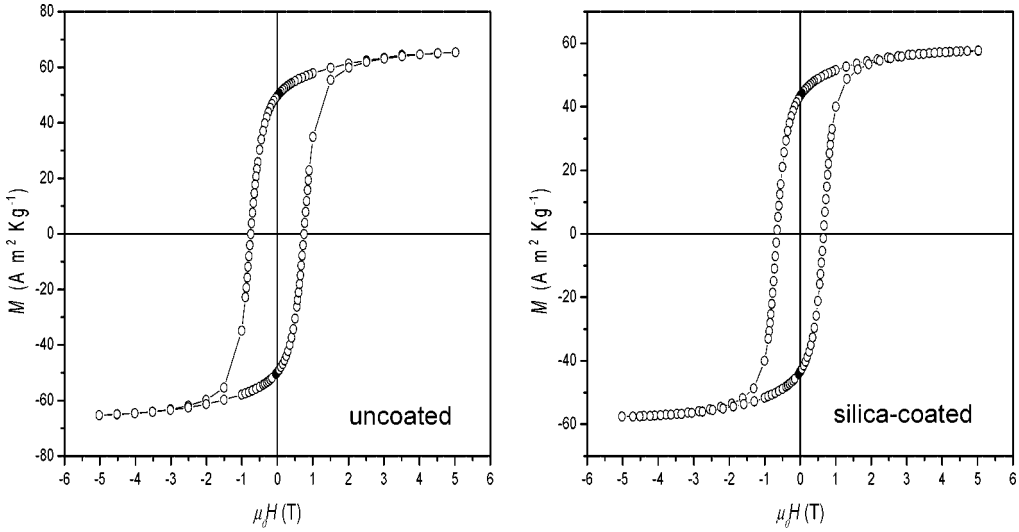

Figure 6. Magnetic hysteresis loop of the uncoated (left side) and coated (right side) $CoFe_2O_4$ sample.

Table 1. Parameters Obtained from Magnetization versus Field Measurements at 5K: Saturation Magnetization (M_s), Reduced Remanent Magnetization (M_r/M_s), and Coercive Field ($\mu_0 H_c$)

	M_s (A m^2 Kg^{-1})	$\mu_0 H_c$ (T)	M_r/M_s
uncoated	67.9(1)	0.75(4)	0.72(2)
silica-coated	58.5(1)	0.66(3)	0.73(2)

the mild synthetic conditions used, the reduction of M_s cannot be ascribed to any potential magnetic coupling of spins at the interface between the magnetic core and the silica shell as observed in other cases.[56] The reduced remanence value (M_r/M_s) does not change significantly from uncoated (0.72) to silica coated nanoparticles (0.73) and the similarity in the shape of hysteresis further confirms that the decrease of M_s in the coated sample is due to the presence of diamagnetic silica.

(56) Aliev, F. G.; Correa-Duarte, M. A.; Mamedov, A.; Ostrander, J. W.; Giersig, M; Liz-Marz*μ*n, L. M.; Kotov, N. A *Adv. Mater.* **1999**, *11, 12*, 1006.

Discussion and Conclusion

Use of the normal micelle method proved to be appropriate for the preparation of clusters of iso-oriented cobalt ferrite nanoparticles. The primary $CoFe_2O_4$ nanocrystals, of about 7 nm in dimension, self-assemble in spherical aggregates of about 50−60 nm in diameter. One can suggest that single particles nucleate at the polar heads of surfactant chains, attracting each other and clinging. The surfactant chains adsorbed at the surface of the primary particles hamper their assembling into a compact single crystal, inducing the formation of a wormlike pores structure inside the spherical aggregates. As a consequence, the continuity of lattice planes in the assemblies is not complete, justifying the differences on the particle size values obtained by the different techniques. The spherical 50–60 nm aggregates can not be seen as a "monocrystals" because the XRD coherent domains are limited by grain boundary and pores. Therefore, the average XRD crystallite size value of 21 nm turns out lower than the diameter of the spherical aggregates; at the same time, it is higher than that of the primary particle size observed

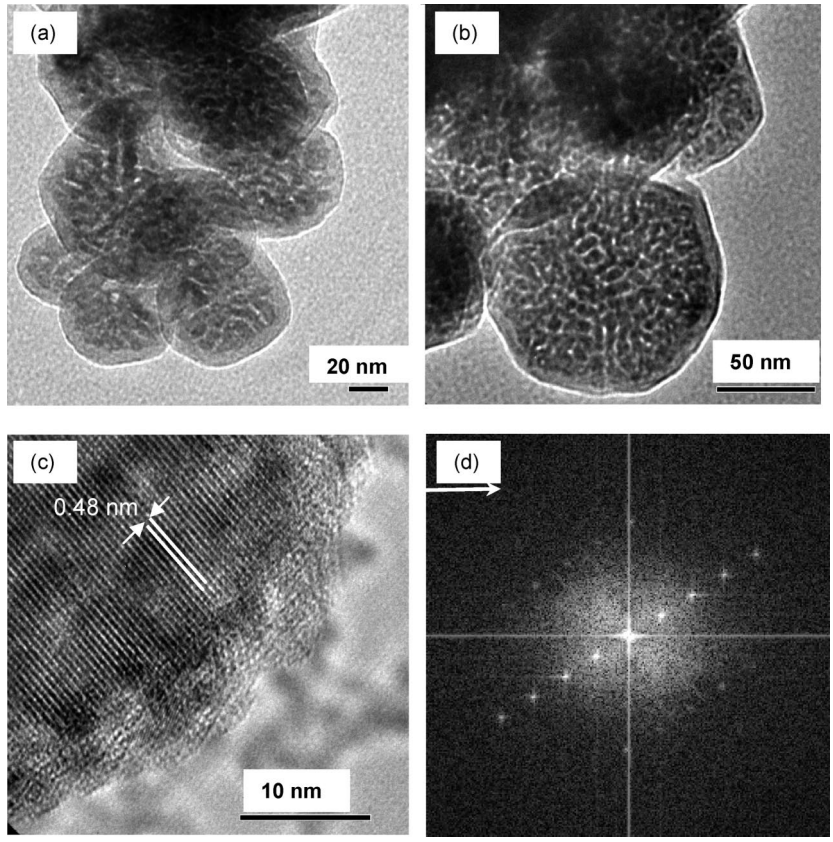

Figure 7. (a−c) HRTEM images and (d) FFT of the silica-coated $CoFe_2O_4$ sample.

by TEM, and confirmed by BET measurements, due also to the presence of twins made up of about 2−3 primary nanoparticles.

Very similar results were presented by Mørup et al.[57] in a study of oriented attachment occurring among α-Fe_2O_3 nanoparticles; the correlation lengths of aggregates from a neutron diffraction peak analysis turned out three times greater than that of primary particles. In further explanation to the results obtained, it was proposed that the attachment of the particles is primarily epitaxial, but twinning of some lattice planes can also take place.

According to the above formation mechanism, the aggregates are porous and possess an extended surface area. The solvents can easily move inside the pores, so that the clusters can be satisfactorily washed and the surfactant completely eliminated, as demonstrated by IR spectra.

The direct micelle route has been used to prepare various ferrite samples, including $CoFe_2O_4$[22,5] in many investigations. Because not all the parameters affecting the characteristics of the products are described in detail, it is not possible to make a complete comparison with these results. The authors claim to have prepared small isolated particles, even though the occurrence of strong magnetic interparticle interactions in pure powders was unavoidable, as revealed by the FC magnetization curves that are typical of strongly interacting systems.

ZFC-FC measurements display strong interactions among particles for both samples and the existence of ferrimagnetic nanoparticles is proved even at room temperature. Saturation magnetization resulted lower than that of bulk $CoFe_2O_4$, but strong enough to move the particles easily by external magnetic forces.[58] This was verified also at room temperature.

Through a reverse micelle method the cobalt ferrite aggregates are efficiently covered by a 7−8 nm thick silica shell. It is important to stress that the covering of nanoparticles by a silica shell has been widely used to coat single particles, rarely aggregates. The adopted procedure does not modify either the structural and morphologic properties or the magnetic ones in any significant way, as attested by XRD patterns, TEM micrographs, and magnetic measurements.

In conclusion, the complete procedure seems to be able to produce aggregates big enough to be "magnetically driven", but small enough to be able to move in biological fluids and to avoid precipitation due to gravitational forces. It looks attractive because its great versatility allows us to modify the characteristics of both the magnetic core and the silica shell.

The size of primary nanocrystals can be modified either at a fixed concentration of the salts by increasing the synthetic temperature and by varying the type of the salt (see the Supporting Information), in addition to the modification of the salt concentration. As a consequence, there is a change in the interactions among particles and in their tendency to aggregate, as well as in the characteristics of clusters.

Likewise, the properties of the silica coating are susceptible to modification. In fact, the thickness of the covering layer and its compactness can be altered by a proper choice of

(57) Frandsen, C.; Morup, S. *J. Phys.: Condens. Matter* **2006**, *18*, 7079.

(58) Lima, E.; Brandi, A. L.; Arelaro, A. D.; Goya, G. F. *J. Appl. Phys.* **2006**, *99*, 083908.

TEOS concentration, reaction temperature and pH of the aqueous phase, where TEOS hydrolysis and polycondensation take place.

Acknowledgment. This work was supported by the University of Cagliari and by the Banco di Sardegna Foundation.

Supporting Information Available: XRD and TEM results on $CoFe_2O_4$ nanoparticles obtained in different synthetic conditions (PDF).This material is available free of charge via the Internet at http://pubs.acs.org.

CM801839S